Sound & Vibration 2026, 60(1), 3785.
doi: https://doi.org/10.59400/sv3785

Article

Sidelobe suppression in loudspeaker line array via sparse optimization

Yuxin Liu, Hui Ren, Zhen Li*, Qian Zhou

School of Information and Communication Engineering, Communication University of China, Beijing 100024, China
*** Corresponding author:** Zhen Li, lizhen78good@126.com

CITATION

Liu Y, Ren H, Li Z, et al. Sidelobe suppression in loudspeaker line array via sparse optimization. Sound & Vibration. 2026; 60(1): 3785. https://doi.org/10.59400/sv3785

ARTICLE INFO

Received: 25 November 2025
Revised: 22 December 2025
Accepted: 12 January 2026
Available online: 4 February 2026

Abstract: Loudspeaker line arrays, widely deployed in venues such as theaters, stadiums, cinemas, and conference halls, are used to achieve uniform sound field coverage and directional control. Due to the spatial sampling effect of the loudspeaker-line-array discrete structure on an ideal continuous line source, periodic sidelobes inevitably appear in the sound radiation directivity pattern, whose pressure level increases with frequency. To mitigate this problem, a sidelobe suppression approach based on sparse array optimization is proposed. To reduce peak side lobe sound pressure levels, particle swarm optimization (PSO) and constrained genetic algorithms (GA) are employed to achieve random sparse optimization of array element positions and sparse optimization of structural symmetry in loudspeaker line array, respectively. Furthermore, due to the increased side lobe sound pressure level after beam steering, a beam steering algorithm combining sparse constraints with an improved Cosh criterion was proposed to achieve effective side lobe suppression following beam steering. This algorithm maintains the sidelobe suppression effect while achieving digital beam steering, allowing the main beam to be directed to a specific direction without requiring mechanical movement. The simulation results indicate that, by sparsifying loudspeaker units, the proposed method effectively suppresses the sidelobe sound pressure levels, with acceptable performance degradation in main-beam gain. In addition, flexible digital beam steering is archived with the sparsely optimized loudspeaker arrays in a low sidelobe level.

Keywords: loudspeaker line array; sparse array; sidelobe suppression; optimization algorithm; beam steering

1. Introduction

Loudspeaker line array have become indispensable acoustic systems in large performance venues, as they achieve radiation characteristics unattainable by individual loudspeakers. Early research by Wolff and Malter [1] on the directivity of point sources, line sources, curved surface sources, and planar sources laid the theoretical foundation for modern array design. In practical applications, multiple loudspeaker units are typically combined to meet the acoustic energy and reverberation requirements of large spaces, leveraging wave superposition and interference principles to enhance overall sound output. However, as frequency increases, the main lobe gradually narrows while side lobes intensify, leading to reduced directivity and energy concentration in the array [2]. Theoretically, significant advances have been made in beamforming and array signal processing, enabling sound focusing, frequency-invariant beamforming, and super-directional beamforming [3–5]. Side lobe suppression has been a focus in fields such as sensor array, ultrasonic array, antenna array, and parametric array

loudspeakers. For sparsely sampled acoustic vector hydrophone mutually orthogonal arrays, Chen et al. [6] proposed an array expansion technique based on the product-minimum method and a combined pressure-velocity processing weighting scheme to suppress side lobes. Wu et al. [7] proposed a projection-based directional coherence factor beamforming method to reduce sidelobes in the full imaging region of ultrasound arrays. Luo et al. [8] employed a dual-substrate integration of suspended-wire serial feed and inverted-T vertical patch structures to achieve a beamwidth expanded to 140 degrees in the H-plane while maintaining low sidelobe levels in the E-plane. Zhu et al. [9] proposed an enhanced beamforming method based on the minimum variance distortionless response algorithm to address the grid lobe issue arising from the short wavelength of multi-channel parametric array loudspeaker arrays. However, existing methods for loudspeaker line arrays have not resolved the issue of reduced energy concentration caused by side lobes. Despite these advancements, the issue of side lobe energy leakage caused by the discrete structure of arrays remains inadequately addressed, particularly when balancing acoustic performance with structural feasibility.

A single loudspeaker struggles to maintain uniform response across the entire frequency range. By combining high- and low-frequency drivers into an array and employing crossover processing with spatially optimized placement of these units, such systems effectively enhance wideband radiation performance. Building upon this, Van Trees [10] proposed a collinear array structure to improve array symmetry. In recent years, speaker array and sound field control technologies have continued to evolve. Ahrens et al. [2] proposed a spatial-frequency-domain-based sound field reconstruction method, while Romoli et al. [11] introduced a low-complexity digital beamforming method based on wavefield synthesis, enabling frequency-independent directional control. Progressive curved line source arrays can achieve specific sound field coverage objectives [12]. Subband adaptive filtering combined with a loudspeaker line array reduces spatial complexity [13]. According to the spatial sampling theorem, beyond the upper frequency limit, simply increasing the number of loudspeakers exacerbates tonal distortion due to spatial aliasing [14]. Jiang et al. [15] introduced head-tracking dynamic dual-channel Ambisonics, significantly reducing requirements for virtual speaker count and HRTF processing complexity. Thus, more speakers in an array do not necessarily equate to better performance; a balanced approach considering both acoustic quality and system efficiency is essential.

Intelligent optimization algorithms, such as genetic algorithms (GA) and particle swarm optimization (PSO), demonstrate significant advantages in various optimization problems, including those involving unmanned aerial vehicles, antenna arrays, and ultrasonic arrays. In the field of unmanned aerial vehicles, Yan et al. [16] employed a spherical vector particle swarm algorithm to plan efficient, low-cost flight trajectories; an enhanced particle swarm algorithm achieved joint optimization of delay and energy consumption in task offloading [17]. Yang et al. [18] employed an improved particle swarm algorithm in reliability-based design optimization (RBDO) under mixed uncertainties to rapidly locate the global optimal most probable point (MPP), effectively mitigating the trade-off between computational efficiency and accuracy. In structural

reliability analysis, the particle swarm optimization algorithm significantly enhanced the precision of reliability analysis by optimizing the hyperparameters of the support vector regression (SVR) model [19]. However, sparse random arrays have yet to be applied in the design of directionally adjustable loudspeaker line arrays, despite successful implementations in antenna arrays and ultrasonic arrays [20]. Haupt [21] pioneered the application of genetic algorithms to sparse synthesis for antenna arrays, representing array element retention and deletion via binary encoding of "1" and "0". Subsequently, Pueo et al. [22] extended antenna array theory to acoustic array pattern design and employed genetic algorithms to optimize phase excitation weights, achieving uniform sound pressure distribution within the linear listening zone [23]. Based on sparse methods, multi-zone sound field reproduction can be further realized [24]. Zhong et al. [25] proposed a sparse random array-based method to optimize element positions and weighting coefficients for suppressing side lobes in ultrasonic arrays. Algorithms for solving sparse array optimal configurations include simulated annealing (SA), genetic algorithms, differential evolution algorithms, and particle swarm optimization [20, 26]. Building upon this, this paper first applies GA and PSO to suppress sidelobes in a directionally adjustable loudspeaker line array.

To address the aforementioned issues, this paper proposes an optimization framework for a loudspeaker line array based on sparse array design. This method employs a particle swarm optimization (PSO) algorithm to achieve side lobe suppression under unconstrained conditions, while further incorporating a constrained genetic algorithm to preserve array symmetry and installation feasibility. Numerical simulations validate the proposed method's effectiveness, demonstrating that this sparse optimization design significantly reduces side lobe energy leakage while preserving main lobe integrity. Building upon this dual-optimization framework, a digital beamforming algorithm combining sparse constraints with an improved hyperbolic cosine (Cosh) criterion is further proposed. This approach enables flexible main beam steering while maintaining low side lobe levels. Numerical simulations demonstrate that this method substantially reduces side lobe energy leakage while preserving main lobe integrity, offering a practical solution for high-performance loudspeaker line array design.

The remainder of this paper is organized as follows. Section 2 formulates the directivity models for both uniform and non-uniform loudspeaker line arrays. Section 3 details the proposed sparse optimization methodologies based on the Genetic Algorithm and Particle Swarm Optimization, alongside a beam-steering algorithm that integrates sparse constraints with an improved Cosh criterion. Section 4 presents numerical simulations to compare the performance of the different algorithms, validating the effectiveness of the proposed approach in sidelobe suppression and beam steering. Finally, Section 5 concludes the work and suggests potential directions for future research.

2. Problem formulation

In a free-field environment, the far-field radiation of a linear loudspeaker array can be modeled as the superposition and interference of point sources. The

resulting radiation pattern consists of a main lobe and multiple sidelobes. When the acoustic wavelength is much larger than the source dimensions, each element may be approximated as a point source, and the sound field at an observation point is obtained by summing their contributions, which can be expressed through multipole expansion.

Consider a pulsating sphere of radius a located at the origin. When $\frac{a}{c_0 \to 0}$, i.e., the geometric size of the sphere is negligible compared to the distance to the observation point, the acoustic pressure and particle velocity distributions in the radiated field can be expressed as

$$p(r,t) = \frac{\rho_0}{4\pi r} q\left(t - \frac{r}{c_0}\right), \tag{1}$$

$$v(r,t) = \frac{1}{4\pi r}\left[\frac{1}{c_0}\dot{q}\left(t - \frac{r}{c_0}\right) - \frac{1}{r} q\left(t - \frac{r}{c_0}\right)\right] e_r. \tag{2}$$

In this case, the infinitesimal pulsating sphere at the origin can be regarded as a point mass source, referred to as a monopole source. Equation (1) describes the pressure distribution, while Equation (2) represents the particle velocity distribution in the radiated field. Together, they define the monopole radiation field, which corresponds to the classical point-source radiation model.

2.1. Directivity of uniform loudspeaker line array

A one-dimensional line array consisting of N point sources is illustrated in **Figure 1**.

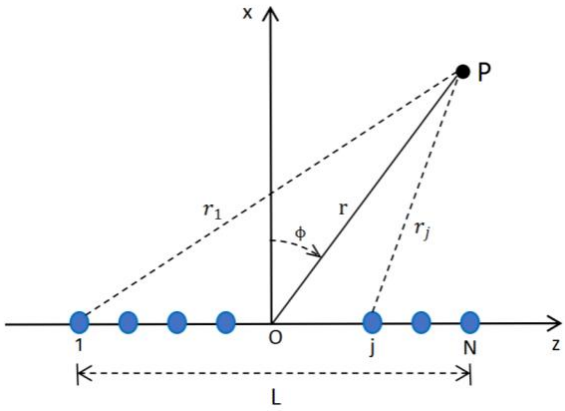

Figure 1. Loudspeaker line array with constant spacing.

In this study, each loudspeaker element is assumed to radiate omnidirectionally and can be modeled as a monopole point source [27]. Accordingly, the total sound pressure distribution of the line array can be expressed as

$$p(r,\varphi,\omega) = \sum_{j=1}^{N} \frac{A}{4\pi r_j} \exp(ik_0 r_j), \tag{3}$$

where $p(r,\varphi,\omega)$ denotes the total pressure. Under far-field conditions, the total array length L satisfies $L = (N-1)I \ll r$, and l represents the spacing between adjacent point sources.

As shown in **Figure 1**, the distance between the *j*-th source and an observation point is r_j, satisfying

$$r_j \approx r_1 - (j-1)\Delta (j = 2, 3, \cdots, N), \tag{4}$$

for $\Delta = l \sin\varphi$, when the array center is taken as the origin, the far-field pressure satisfies

$$p(r, \varphi, \omega) \approx \frac{A}{4\pi r} e^{ik_0 r} \frac{\sin(Nk_0\Delta/2)}{\sin(k_0\Delta/2)}, \tag{5}$$

where N is the number of array elements, A denotes the amplitude weight of each element, $k_0 = 2\pi/\lambda$ is the wavenumber, and λ is the wavelength. When $\varphi = 0$, the far-field pressure reduces to

$$p(r, \varphi, \omega) = p(r, 0, \omega) D(\varphi), \tag{6}$$

where $D(\varphi)$ is defined as the directivity factor, or array factor, given by

$$D(\varphi) = \frac{\sin(Nk_0 l \sin\varphi/2)}{N \sin(k_0 l \sin\varphi/2)}. \tag{7}$$

The normalized array factor is expressed as

$$D(\varphi)_N = \left| \frac{D(\varphi)}{\max(D(\varphi))} \right|, \tag{8}$$

and the corresponding normalized sound pressure level (SPL) curve is given by

$$SPL(\varphi) = 20\, lg\, D(\varphi)_N. \tag{9}$$

To avoid grating lobes, the element spacing d must satisfy the condition

$$d < \frac{\lambda}{2}. \tag{10}$$

This study focuses on mid- to high-frequency line arrays operating at frequencies up to 2500 Hz. For a wavelength $\lambda = c_0/f = 343/2500 \approx 0.1372$ m, Equation (10) indicates that $d < 0.0686$ m. Considering a mid- to high-frequency loudspeaker of 2-inch diameter (≈ 0.052 m), the element spacing d should satisfy

$$0.0520 < d < 0.0686. \tag{11}$$

Accordingly, a practical element spacing of $d = 0.06\ m$ is selected for the line array in this study.

2.2. Directivity of non-uniform loudspeaker line array

Non-uniform linear loudspeaker arrays can be classified into three types: non-uniform element spacing, non-uniform excitation amplitude, and non-uniform excitation phase progression. An array is considered non-uniform if it satisfies any one of these conditions. An example of a linear loudspeaker array with non-uniform element spacing is illustrated in **Figure 2**.

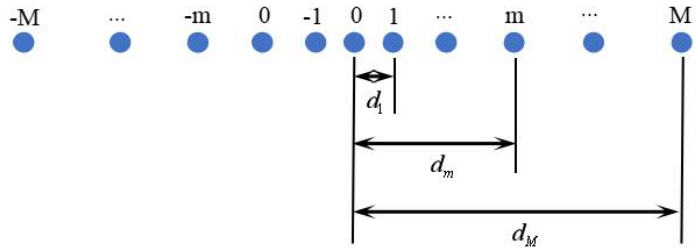

Figure 2. Symmetrical loudspeaker line array with non-uniform element spacing.

Let the array element spacing increment factor be denoted as a, where $1 \leq a \leq 1+\delta, \delta = 0 \sim 0.2$; thus, the relationship is given by

$$d_m = d_{m-1} + a\left(d_{m-1} - d_{m-2}\right) = \left(\sum_{n=0}^{m-1} a^n\right) d. \tag{12}$$

Let $d_m = \varsigma_m d$, where $\varsigma_m = \sum_{n=0}^{m-1} a^{x_n}$ denotes the spacing factor, and $x_n = n$ or $x_n = kn$ with $k < 1$, as expressed in the equation.

Therefore, the number of array elements is $N = 2M + 1$. The directivity factor of a symmetric linear loudspeaker array with an odd number of elements, nonuniform spacing, and unequal amplitude distribution is given as

$$D(\varphi) = A_0 + \sum_{m=1}^{M} A_m \left[e^{-j(kd_m\ cos\ \theta\ +\ \alpha_m)} + e^{j(kd_m\ cos\ \theta\ +\ \alpha_m)}\right] = A_0 + 2\sum_{m=1}^{M} A_m\ cos\ \ (kd_m\ cos\ \theta + \alpha_m). \tag{13}$$

3. Methods

The objective of the proposed method is to design a sparse linear loudspeaker array with controllable beam steering capability, such that the radiated acoustic energy is primarily concentrated within the main lobe while minimizing the sidelobe level. The implementation is carried out in three stages: (1) a sparse array design method based on the GA is first investigated, followed by an extended approach employing the PSO algorithm; (2) for arrays with symmetric configurations, a GA-based sparse optimization method is developed to further simplify the array structure and reduce hardware complexity while maintaining acoustic performance; (3) a hybrid algorithm is subsequently introduced, which enables effective beam steering while significantly suppressing sidelobe levels, thereby enhancing the directivity and radiation performance of the array.

3.1. Research on sparse optimization of loudspeaker line array based on genetic algorithm

To achieve the proposed sparse optimization of loudspeaker line array, this study adopts a genetic algorithm (GA) as the core optimization framework. GA is a global optimization and adaptive probabilistic search technique inspired by the principles of natural selection and genetic evolution.

The optimization process begins with an initial population of candidate array configurations, each evaluated using a fitness function designed to quantitatively

reflect the acoustic performance objective of sidelobe suppression. Through iterative genetic operations—including the selection of high-fitness individuals, crossover to combine advantageous traits, and mutation to maintain population diversity—the algorithm progressively evolves toward an optimal configuration. Previous studies have indicated that the quality of population initialization exerts a significant influence on the optimality of the final solution [28].

The design of the GA in this study includes careful consideration of encoding schemes for array element distributions, construction of a problem-specific fitness function, tailored genetic operators, and appropriate control parameter settings [29]. This approach provides the foundation for the subsequent development of sparse optimization strategies, including symmetric array optimization and hybrid algorithms for beam steering and sidelobe suppression.

In this study, a 40-element loudspeaker line array was sparsified into a 34-element configuration, corresponding to a sparsity ratio of 0.85. The optimization process was implemented using GA. The simulation parameters were set as follows: the population size was $N_p = 50$, the gene dimension of each individual was $L = 40$, and the maximum number of generations was $G = 200$, The crossover probability and mutation probability were denoted as $P_c = 0.8$ and $P_m = 0.05$, respectively.

A binary initial population was randomly generated, where each chromosome contained a fixed number of active elements (encoded as "1") corresponding to the desired sparsity ratio. The fitness function of each individual was evaluated according to the beamforming performance criterion and subsequently normalized. Based on the fitness distribution, the roulette-wheel selection strategy was adopted to select parent individuals. New offspring were then generated through probabilistic crossover and mutation operations with rates P_c and P_m.

To preserve the sparsity structure, the number of active elements in each new individual was constrained to remain constant. The elitist strategy was employed to retain the best-performing individuals across generations. The algorithm iteratively updated the population until the termination condition was met. If the convergence criterion was satisfied, the search process was terminated, and the optimal sparse configuration was obtained; otherwise, the GA continued the evolutionary optimization. The procedure of this algorithm is summarized in **Algorithm 1**.

Algorithm 1. Genetic algorithm.

Input: N_P, L, G, P_c, P_m, f, c_0, d, $lamda$, $seta_0$, NL.
Output: fBest
Generate the initial population f_0.
for *g* = 1:G
Calculate the fitness of an individual *Fit*(*i*).
Fit = (*Fit-minFit*)/(*maxFit-minFit*).
Replication operation based on roulette wheel.
Crossover operation based on probability $P_c = 0.8$.
Mutation operation based on probability $P_m = 0.05$.
Adjust the actual number of array elements of individuals in the population while keeping $NL = 34$ unchanged.
f(;1) = fBest.

The fitness function is employed to evaluate the performance of each individual and is typically constructed according to the specific optimization objectives of the problem. In this study, the positions of the loudspeaker array elements are defined as the decision variables, and a binary encoding scheme is adopted to represent the spatial distribution of the elements along the linear array. The fitness function is formulated with the objective of minimizing the sidelobe sound pressure level (SPL) of the loudspeaker line array.

For a uniformly spaced linear loudspeaker array, sparsity optimization is achieved by introducing a binary variable f_m to indicate the presence state of the *m*-th element. Specifically, $f_m = 1$ represents that a loudspeaker element is active at the corresponding position, whereas $f_m = 0$ indicates that the element is inactive, i.e., removed through sparsification. Accordingly, the corresponding radiation directivity function of the sparse array can be expressed as

$$p(\theta) = \sum_{m=0}^{N-1} e^{j\frac{2\pi}{\lambda} d_m (sin\ \theta - sin\ \theta_0)} \cdot f_m, \tag{14}$$

where θ_0 is the beam deflection angle, and α_m is the phase compensation required for the array elements to achieve this deflection. The relationship between them is given by

$$\alpha_m = k d_m\ sin\,(\theta_0)\,. \tag{15}$$

Based on the definition of the maximum sidelobe level in the radiation directivity pattern of the loudspeaker line array, the corresponding optimization model can be formulated as

$$\min_f MS = \min_f \max_{\theta \in S} \{p_{dB}(\theta)\} = \min_f \max_{\theta \in S} \left\{ 20\ lg \frac{p(\theta)}{max\,(p(\theta))} \right\}. \tag{16}$$

Here, $max(\cdot)$ denotes the maximum value function, and $p_{dB}(\theta)$ represents the normalized radiation directivity function of the loudspeaker array. The symbol S defines the sidelobe region of the radiation pattern.

If the zero-power points of the main lobe are located at $2\varphi_0$, then the sidelobe region $S = \{\theta | \theta_{\min} \le \theta \le \theta_0 - \varphi_0 \cup \theta_0 + \varphi_0 \le \theta \le \theta_{\max}\}$.

3.2. Research on sparse optimization of loudspeaker line array based on particle swarm optimization algorithm

The PSO algorithm is characterized by its intuitive concept and relatively simple computational procedure. In this study, the optimization of a 40-element loudspeaker line array is performed simultaneously. Specifically, a set of particles is defined, corresponding to the 40 array elements, with 34 elements randomly assigned a value of 1 in a one-dimensional space to represent the active loudspeaker positions, thereby forming an initial candidate solution. Each particle's position is then evaluated according to its ability to address the optimization problem. Subsequently, the particles

update their positions following stochastic or deterministic rules, generating new candidate solutions that are re-evaluated. During the iterative process, each particle records its own best position, referred to as the local best, while also being informed of the global best position identified among the entire swarm. Through continuous oscillation and stochastic adjustment, the swarm collectively converges towards the vicinity of the global optimum, where the search process eventually terminates [30,31].

In this study, the loudspeaker line array consists of 40 elements. Accordingly, the initial particle swarm size is set to 50. The array configuration is represented by assigning the value 40 to the loudspeaker element positions, and a random function is employed to generate candidate solutions within the interval [1], from which 34 active elements are selected to form the sparse array. The complete procedure of this algorithm is summarized in **Algorithm 2**.

Algorithm 2. Particle swarm optimization algorithm.

Input: N_P, L, G, w, c_1, c_2, f, c_0, d, $lamda$, $seta_0$, NL.
Output: xmBest.
Generate the initial population f_0.
for *k* = 1:G
Calculate the fitness of an individual *Fit*(i).
Find the global optimal particle.
for 1:NP
for
Particle velocity update.
Particle position update.
Keep the actual number of array elements NL unchanged.
Update the optimal group.
Update the optimal individual *xm*.

The inertia weight is set to 0.3, while the cognitive and social learning factors are set to 0.3 and 0.2, respectively. For consistency and comparative analysis, the number of PSO iterations is fixed at 200, identical to that of the genetic algorithm. During the optimization process, the particles are iteratively updated in an N-dimensional space, with their velocities and positions adjusted according to the defined update rules, while ensuring that the number of active elements remains constant. At each new position, the fitness function is evaluated by calculating the sidelobe levels of the radiation pattern. After 200 iterations, the swarm converges to a local optimum corresponding to the minimum sidelobe level. By repeating this iterative process, the algorithm progressively approaches the global optimum, thereby minimizing the sidelobe radiation of the array.

Considering the inherent defects in actual manufacturing and installation processes, independent random position perturbations are introduced for each array unit, with a maximum displacement constraint of 5% of the unit spacing. A “position tolerance robustness penalty term” is incorporated into the PSO fitness function to penalize sensitivity to unit position perturbations.

$$\Delta x_n \sim u(-0.05d, 0.05d), \tag{17}$$

$$J_{pos} = MS - \alpha_{pos} \cdot \mathrm{Var}\left\{MS_{pos}\right\}. \tag{18}$$

Here, $\alpha_{pos} = 0.5$ is the positional robustness weight.

In addition, random excitation amplitude perturbations are incorporated to model loudspeaker sensitivity mismatches, where the amplitude errors are uniformly distributed within 5%–10%.

$$\Delta a_n \sim u(-\varepsilon, \varepsilon), \tag{19}$$

$$J_{amp} = MS - \alpha_{amp} \cdot Var\left\{MS_{amp}\right\}. \tag{20}$$

Here, $\alpha_{amp} = 0.5$ is the amplitude robustness weight. Through Monte Carlo simulations, both element amplitude errors and position perturbations are simultaneously introduced, and array structures with large performance fluctuations after perturbation are penalized.

$$J = MS - \alpha \cdot Var\left\{MS_{amp+pos}\right\}. \tag{21}$$

Here, $\alpha = 0.5$ is the joint robustness weight.

3.3. Research on symmetric sparse linear loudspeaker arrays based on genetic algorithm

By applying a genetic algorithm (GA) to a 40-element uniformly spaced linear loudspeaker array, sparse optimization can be achieved with the dual objectives of reducing the number of active loudspeaker units and lowering system cost, while simultaneously suppressing sidelobe levels in the directivity pattern. The optimization is further constrained by maintaining a constant array aperture and enforcing symmetrical distribution across the left and right halves of the array.

For a uniformly spaced linear loudspeaker array, sparsity optimization is achieved by introducing a binary variable f_m to indicate the existence state of the corresponding loudspeaker element. Specifically, $f_m = 1$ represents that a loudspeaker element is present at the corresponding position, whereas $f_m = 0$ indicates that the element is absent. Accordingly, the directivity function of the array can be expressed as follows.

$$\min_{f} \max_{\theta \in S} \left\{p_{dB}(\theta)\right\} = \min_{f} \max_{\theta \in S} \left\{\left|\frac{p(\theta)}{max\left(p(\theta)\right)}\right|\right\}. \tag{22}$$

Meanwhile, the following constraints must be satisfied: the linear loudspeaker array should contain active elements at both ends, and the left and right halves of the array must be symmetrically distributed. In addition, the overall array aperture is required to remain constant

$$\begin{cases} f(1) = 1 \\ f(end) = 1 \\ f\left(1:1:\dfrac{end}{2}\right) = f\left(end:-1:\dfrac{end}{2}+1\right) \end{cases} \tag{23}$$

In Equation (22), subscriptsanddenote the existence states of the loudspeaker elements located at both ends of the linear array, respectively. The optimization model remains consistent with the one described previously, where the optimization is performed by adjusting the values of to determine the optimal element positions. The objective is to minimize the maximum sidelobe sound pressure level of the array's directivity pattern while simultaneously satisfying the imposed constraints. The complete procedure of this algorithm is summarized in the following algorithm.

3.4. Beam steering algorithm combining sparse constraints and an improved cosh criterion

Based on the algorithms introduced in the previous three subsections, this study proposes a beam-steering algorithm that combines sparse constraints with an improved hyperbolic cosine (Cosh) criterion. The **Algorithm 3** optimizes the radiation pattern of the loudspeaker line array by simultaneously adjusting and weighting three key parameters.

Algorithm 3. Constrained genetic algorithm.

Input: N_P, L, G, P_c, P_m, f, c_0, d, $lamda$, $seta_0$, NL.
Output: fBest.
Generate the initial population f_0. All individuals in the initial population are in the left half (or right half).
for *g* = 1:G
Calculate individual fitness *Fit*(*i*).
Replication operations based on roulette.
Crossover operation based on probability P_c.
The mutation operation is based on probability P_m.
Symmetrically replicate the half array to obtain the full array.
Adjust the actual number of array elements NL of each individual in the population to remain unchanged, and maintain the symmetry of the left and right half-arrays.
f(;1)=fBest.

Specifically, the process begins with symmetric sparse optimization of the element positions in a uniform loudspeaker line array using **Algorithm 3**, while keeping the delay and input voltage amplitude of each element unchanged. Initially, all element delays are set to zero, and voltage amplitudes are uniformly weighted with a value of 1. The corresponding radiation pattern is then calculated based on the principles of wave superposition and interference, ensuring that the main lobe initially points along the normal direction of the array, thereby establishing a zero-degree initial steering angle.

Subsequently, an improved Cosh algorithm is applied to weight the voltage amplitudes of each loudspeaker element, while preserving the symmetric sparse configuration of the array and taking the array's steering angle into account. The improved hyperbolic cosine (Cosh) algorithm is expressed as

$$A(x_0) = 1 - \frac{\cosh(x_0)}{2}, \tag{24}$$

$$R(\theta) = \int_{-L}^{L} \left[1 - \frac{cosh\,(x_0)}{2}\right] e^{-jkx\ sin\ \theta} dx = \frac{1}{\theta}\ sin\ L\theta + \frac{j}{2(j\theta+1)} sin(j\theta L + L) - \frac{j}{2(j\theta-1)} sin(j\theta L - L). \quad (25)$$

In Equations (24) and (25), x_0 represents the coordinates of the loudspeaker elements, L denotes the length of the loudspeaker array, and θ indicates the steering angle of the array.

As shown in Equation (24), the improved Cosh algorithm is entirely determined by the physical spatial coordinates x_0 of the loudspeaker array elements. Unlike traditional Cosh weighting based on the shape parameter α, this method does not introduce an additional hypercosine parameter α; the weighting shape is inherently determined by the array geometry. Consequently, the improved Cosh algorithm eliminates the need for complex optimization or trade-offs of α for different frequencies or beam directions. Since it contains no frequency-dependent variable parameters, the weighting characteristics remain stable across the entire operating frequency band. Amplitude weighting is responsible for shaping the beam and suppressing side lobes. Meanwhile, the beam's electronic deflection, as shown in Equation (26), is controlled by independently applied delays determined by the physical spatial coordinates *x* of the speaker array elements.

Finally, the main beam of the loudspeaker array can be steered to the desired angle by applying an arithmetic phase delay to each loudspeaker element.

$$\theta = arcsin\left(\frac{x}{d}\right) = arcsin\left(\frac{ct}{d}\right). \quad (26)$$

In Equation (26), *x* corresponds to the propagation distance delay of a given element relative to other elements whose initial delay is set to zero. Here, c denotes the speed of sound in the medium, and *t* represents the applied time delay. The flowchart of the proposed joint algorithm is illustrated in **Figure 3**.

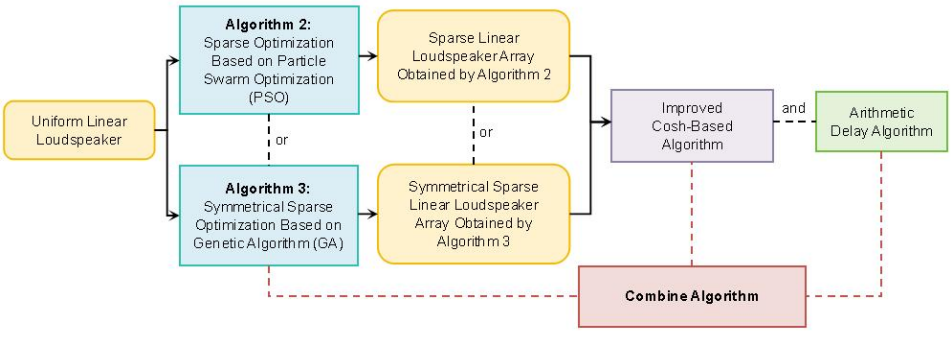

Figure 3. Block diagram of the beamforming algorithm based on joint sparse constraint and improved Cosh criterion.

4. Simulations

Numerical simulations were performed to comprehensively evaluate the radiation directivity of the loudspeaker line array and to compare the results with those obtained using the algorithm presented in Section 3. The simulation results indicate that the proposed method achieves frequency-independent sidelobe suppression

while maintaining high mainlobe steering accuracy. Moreover, under sparse array configurations, the adaptability of the radiated sound field across the entire frequency range was assessed. To further demonstrate the algorithm's capability in beam control and sidelobe suppression, directivity patterns were analyzed at multiple sampled frequencies. All simulations were conducted in a free-field environment to rigorously validate the intrinsic performance of the proposed method.

4.1. Directivity simulation of loudspeaker line array

The loudspeaker line array in this study consists of 40 equally spaced elements. Since the loudspeaker units considered herein are omnidirectional, they can be modeled as point sources. In this representation, a value of 1 on the vertical axis indicates the presence of a loudspeaker element at that position, while a value of 0 indicates its absence. In **Figure 4**, the positions of all 40 array elements are depicted as discrete points.

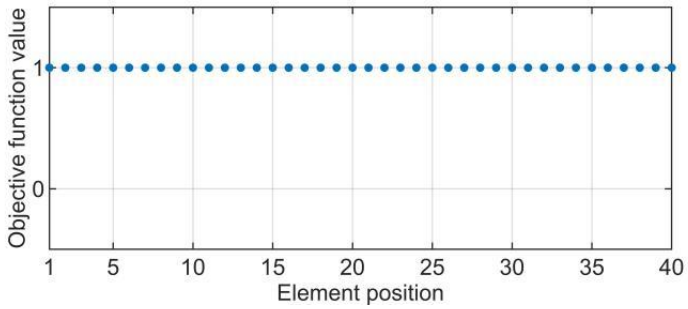

Figure 4. Element position distribution of the loudspeaker line array.

To evaluate the sound field radiation characteristics of the original 40-element loudspeaker line array across different frequencies, a sound field simulation analysis was performed. **Figure 5** presents the normalized sound pressure level (SPL) directivity patterns of the array at 160 Hz, 320 Hz, 640 Hz, 1280 Hz, 1640 Hz, and 2560 Hz.

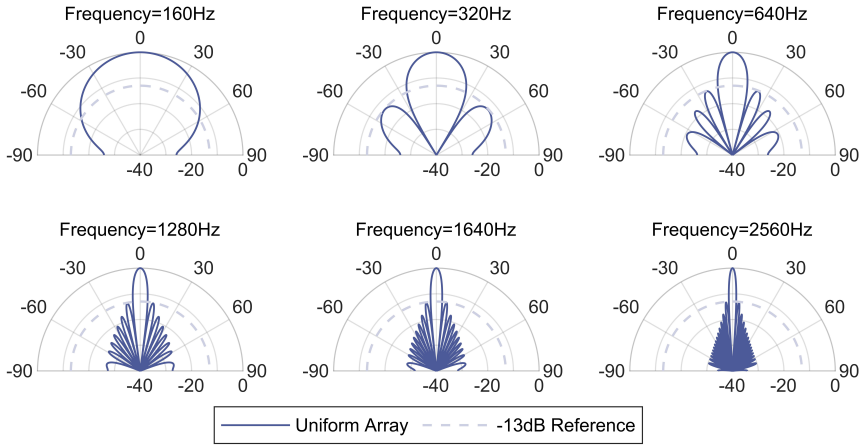

Figure 5. Normalized SPL curve of loudspeaker line array.

The simulation results indicate that, as the excitation frequency increases, the main lobe of the loudspeaker line array's radiation pattern gradually narrows, exhibiting stronger spatial focusing. However, the number of sidelobes also increases

significantly, and the sound pressure level of the first sidelobe rises markedly with frequency, leading to a degradation in the overall directivity performance of the array. For a uniformly distributed line array, the fixed inter-element spacing tends to generate high-amplitude sidelobes at higher frequencies. Such sidelobe structures cause spatial dispersion of acoustic energy, reducing the energy concentration in the main lobe region and adversely affecting the uniformity and clarity of the sound field within the listening area.

Therefore, side lobe suppression directly determines the performance of electroacoustic arrays in practical applications. To address this issue, the array's geometric configuration (such as element spacing and layout) or its complex excitation weights can be optimized. This optimization effectively reduces side lobe levels, concentrating acoustic energy toward the main lobe direction. This significantly enhances the directivity index and beam control precision. Ultimately, in acoustic spaces, robust side lobe suppression is indispensable for achieving exceptional speech intelligibility, high-fidelity music reproduction, and overall system stability—ensuring the system's ultimate performance.

4.2. Simulation of sparse optimization for a loudspeaker array based on a genetic algorithm

The original 40-element loudspeaker line array was sparsely optimized in terms of both element number and positions, ultimately retaining 34 elements, corresponding to a sparsity ratio of 0.85. To achieve an optimal sparse configuration, a binary-encoded genetic algorithm (GA) was employed to optimize the array. Certain parameters were fixed as listed in **Table 1**. Subsequently, the fitness value of each individual was calculated and normalized. Individuals with higher fitness values were selected for reproduction based on a roulette-wheel selection strategy. Genetic recombination and perturbation operations were then performed according to predetermined crossover and mutation probabilities to generate a new population for the next generation.

Table 1. Simulation parameters.

Symbol	Definition	Value
N_p	Initialize the population number	50
L	Individual gene dimension	40
G	Maximum number of evolutionary iterations	200
P_c	Cross probability	0.8
P_m	Mutation probability	0.05
NL	The number 1 in each individual of the population	34

To ensure consistency with the sparsity constraint, structural correction was applied to newly generated individuals after crossover and mutation operations, maintaining a constant number of "1" in each individual and thereby preserving the predetermined array sparsity. Simultaneously, to prevent the loss of the global optimum during evolution, an elitist strategy was employed, whereby the best individual from the current generation was directly carried over to the next generation. This genetic evolution process was iteratively performed until the termination criteria were met,

ultimately yielding the optimal sparse array configuration along with its corresponding objective function value.

The proposed genetic algorithm-based sparse optimization method was validated through simulation. By designing and optimizing the fitness function, the positions of the loudspeaker elements were effectively adjusted to minimize the maximum sidelobe level of the array's radiation pattern. The resulting sparse configuration of the loudspeaker array is shown in **Figure 6**, where a "1" in the binary encoding indicates that the element is retained at the corresponding position, while a "0" indicates that the element has been removed, i.e., no loudspeaker is installed at that position.

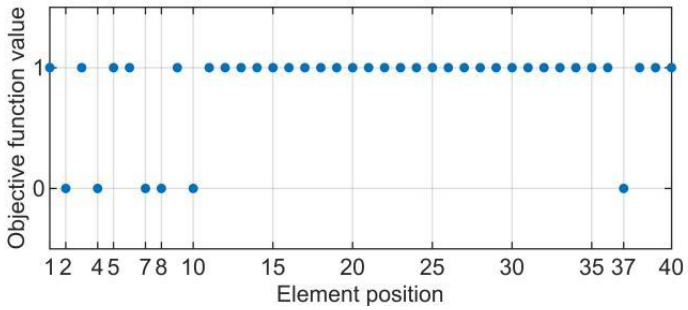

Figure 6. The position of the loudspeaker line array element is optimized by a genetic algorithm.

Figure 7 presents the normalized sound pressure level (SPL) directivity patterns to evaluate the radiation performance of the optimized array across different frequencies. After applying the genetic algorithm to sparsely optimize the original 40-element array, a configuration of only 34 elements with a non-uniform distribution was obtained. The simulation results demonstrate that this optimized array maintains robust main-lobe characteristics while achieving significant sidelobe suppression over a wide frequency range, effectively mitigating the periodic interference effects inherent in a regular array.

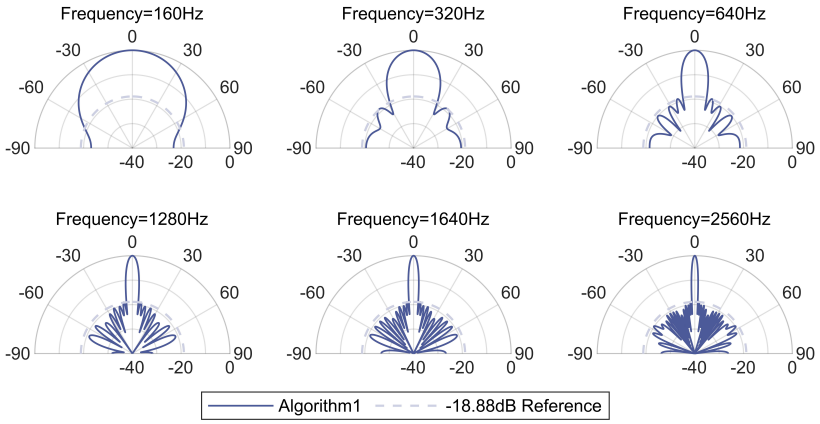

Figure 7. The normalized SPL curve of the loudspeaker line array optimized by the genetic algorithm.

4.3. Simulation of sparse optimization for a loudspeaker array based on particle swarm optimization

In this study, the fitness function used for the PSO is identical to that employed for the genetic algorithm (GA), and both methods utilize the same binary-initialized

population. In both algorithms, the positions of the loudspeaker array elements serve as the decision variables, with the objective of minimizing the sidelobe levels in the array's radiation pattern. The initial population is binary-encoded, where each particle or individual represents a possible sparse configuration of the array: a "1" indicates a retained element, while a "0" indicates an empty position. The resulting sparse configuration of the loudspeaker line array based on the PSO algorithm is illustrated in **Figure 8**.

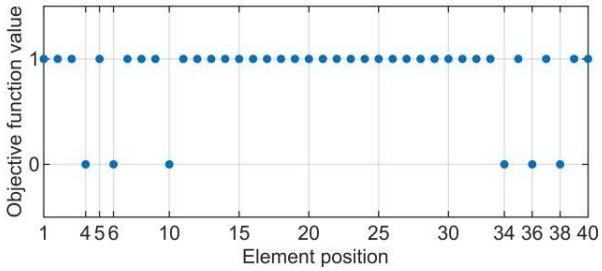

Figure 8. The position of the element is optimized by Particle swarm optimization.

Similar to the genetic algorithm, the PSO was applied to sparsely optimize the original 40-element loudspeaker line array, reducing it to 34 elements. This optimization achieved an improved spatial configuration of the array elements, thereby enhancing the sound field distribution in the radiation pattern. To ensure a fair comparison, both PSO and GA employed the same fitness function and were set to the same maximum iteration count of 200. The proposed genetic algorithm-based sparse optimization method was validated through simulation. **Figure 9** presents the normalized sound pressure level (SPL) directivity patterns.

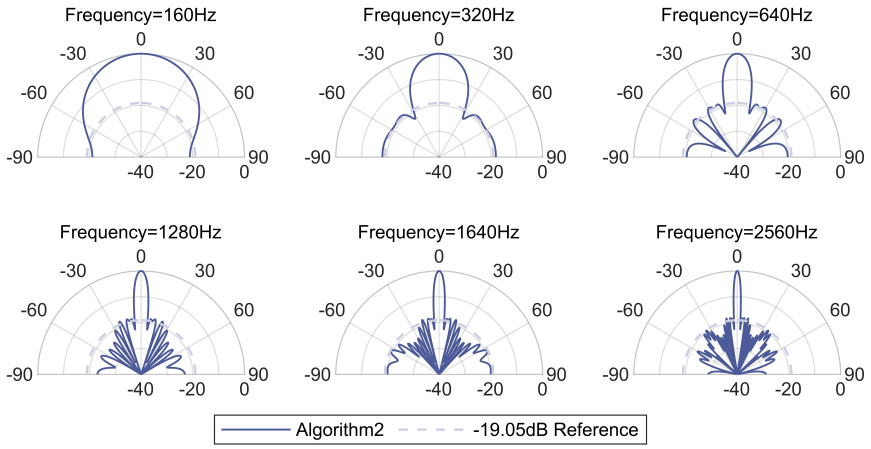

Figure 9. The normalized SPL curve of the loudspeaker line array optimized by Particle swarm optimization.

Following optimization via the particle swarm algorithm, the number of elements in the loudspeaker line array was reduced from the original 40 to 34, matching the sparsity achieved with the genetic algorithm. It is noteworthy that the element positions obtained through PSO differ from those produced by GA, indicating that the two optimization strategies explore the solution space along distinct paths and may converge to different local optima. As shown in **Figure 9**, the PSO-optimized array exhibits a

well-defined and concentrated main lobe across multiple frequencies, while achieving effective sidelobe suppression. Specifically, the normalized sound pressure level curves of the optimized array indicate that the maximum sidelobe level is suppressed below −19.05 dB, demonstrating superior sidelobe control compared to the results obtained via GA.

4.4. Comparative analysis of fitness curves and robustness evaluation of sparse optimization based on particle swarm optimization

To evaluate the convergence properties and stability of different sparse optimization algorithms, this paper conducts a comparative analysis of the fitness evolution processes between sparse optimization methods based on genetic algorithms and those based on particle swarm optimization. **Figure 10** presents the average fitness curves obtained from multiple independent runs under identical initial conditions and optimization objectives.

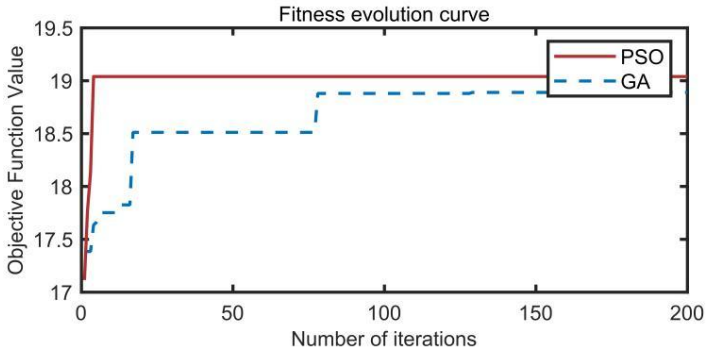

Figure 10. Fitness convergence curves of GA and PSO for sparse optimization of a 40-element loudspeaker line array.

As shown in **Figure 10**, the PSO algorithm converges to the optimal solution after only six iterations, whereas the GA requires approximately 185 iterations to reach convergence. In comparison, GA exhibits longer computation times and slower iteration speed during the search process, while PSO demonstrates stronger convergence performance and higher optimization efficiency.

When the loudspeaker line array is expanded to consist of 100 omnidirectional units distributed at equal intervals, the method described in Section 2 yields d=0.06 m. Keeping all other conditions constant, the number of units selected in the sparse loudspeaker line array is 85. **Figure 11** illustrates the fitness convergence behavior of the Genetic Algorithm (GA) and Particle Swarm Optimization (PSO) as the number of iterations increases for the 100-element array configuration.

The corresponding results for the 100-element array are presented in **Figure 11**. With the increased problem dimensionality, both algorithms require more iterations to converge. Nevertheless, PSO still converges considerably faster, reaching convergence after approximately 19 iterations, while GA requires about 136 generations to achieve a comparable fitness level. Importantly, no reversal of the relative convergence trend between the two algorithms is observed when the array size is increased from 40 to 100 elements. PSO can further reduce side lobe energy while maintaining main lobe directivity and energy focusing capability, thereby enhancing the spatial concentration

of acoustic energy.

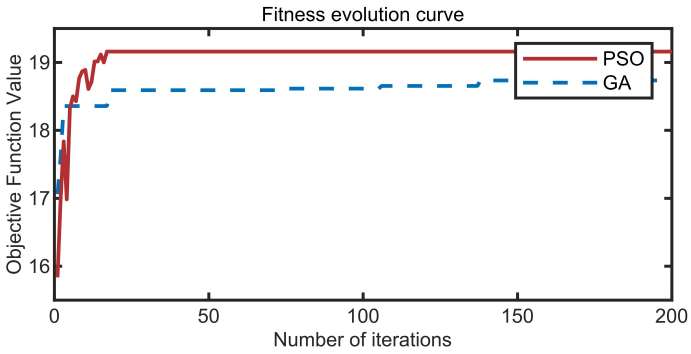

Figure 11. Fitness convergence curves of GA and PSO for sparse optimization of a 100-element loudspeaker line array.

In the robustness analysis, defects inherent in the actual manufacturing and installation processes were taken into account. Based on Equations (17)–(21), Monte Carlo simulations were conducted to perform a statistical evaluation of the array's sidelobe suppression performance. The sensitivity curve of peak side lobe level to manufacturing errors of the array elements is shown in **Figure 12**.

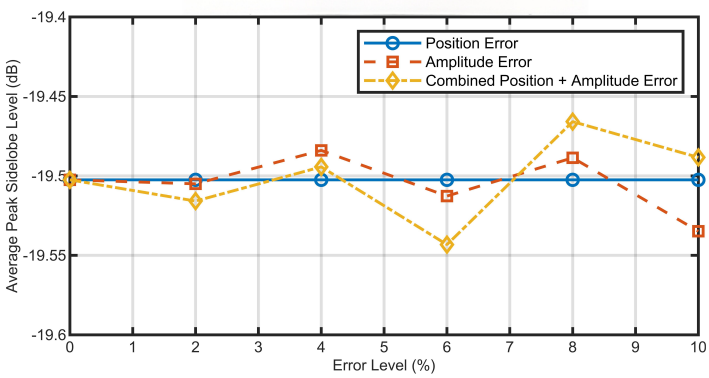

Figure 12. Sensitivity of peak sidelobe level to manufacturing errors.

The results indicate that the resulting degradation in side lobe SPL performance is extremely limited. Specifically, the average side lobe SPL variation consistently remained within the range of 0.05–0.15 dB relative to the nominal array. No monotonic deterioration trend was observed as the amplitude error level increased; fluctuations primarily exhibited random characteristics. **Figure 12** demonstrates that the proposed scheme exhibits inherent robustness to moderate amplitude variations under the considered array configuration and side lobe suppression targets.

4.5. Simulation of symmetric sparse optimization for loudspeaker line array via genetic algorithm

This study systematically analyzed the constrained genetic algorithm-based sparse optimization of loudspeaker line arrays from three perspectives: the optimized element position distribution, the directivity patterns at key frequencies, and the convergence of the fitness function. By optimizing the spatial distribution of array elements, the original 40-element line array was sparsely reduced to 34 elements, while strictly retaining the elements at both ends to ensure that the overall array aperture remained

unchanged. Additionally, during the optimization process, the left and right subarrays were constrained to maintain symmetric distributions, preserving the array's radiation characteristics and sound field balance.

Figure 13 illustrates the distribution of the optimized array elements, highlighting the structural adjustments achieved through sparse optimization. At each iteration, the fitness value was calculated based on the element positions of the current individual, and the genetic algorithm's evolutionary operations were applied to iteratively seek the optimal configuration. The resulting array achieved the lowest maximum sidelobe level.

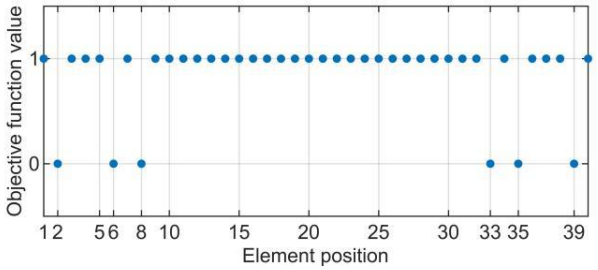

Figure 13. The position of the element is optimized by Particle swarm optimization.

As the number of iterations increases, the elements removed from the constrained genetic algorithm-based line array are continually adjusted, resulting in progressively changing element arrangements. This iterative process continues until the optimal sparse configuration of the line array is identified, achieving the best sidelobe suppression. The directivity patterns of the symmetric, sparsely optimized line array based on the genetic algorithm are shown in **Figure 14**.

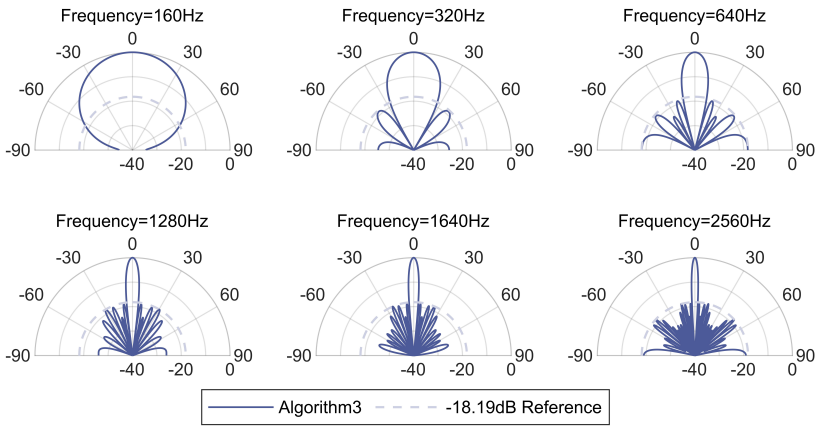

Figure 14. Directivity pattern after genetic algorithm-based symmetric sparse optimization.

The application of a genetic algorithm under the imposed constraints enabled the sparse optimization of the loudspeaker line array, reducing the number of elements from 40 to 34. The resulting normalized sound pressure level (SPL) directivity patterns across multiple frequencies, shown in **Figure 14**, demonstrate a well-defined main lobe and effective sidelobe suppression. More importantly, the maximum sidelobe level is consistently maintained below −18.19 dB over all tested frequency bands. Under the considered asymmetric observation geometry, the enforced left-right mirror symmetry leads to an additional sidelobe level change of approximately 1 dB. In practical sound

reinforcement applications, a 1 dB increase in the peak sidelobe level generally has a negligible perceptual impact.

Notably, in this optimization scheme, the elements at both ends of the array are retained, and the left and right subarrays remain strictly symmetric. This design simultaneously satisfies the constraints of structural symmetry and constant aperture, while achieving effective sidelobe suppression. These results demonstrate that the proposed constrained genetic algorithm can enhance the main-lobe energy focusing while effectively reducing sidelobe energy leakage, thereby improving the directional control and spatial coherence of the sound field.

4.6. Simulation of beam steering algorithm with sparse constraint and improved cosh criterion

When the sparsely optimized loudspeaker line array undergoes beam steering, the sidelobe suppression performance tends to degrade as the frequency increases. To address this issue, a phase-delay and amplitude-weighting strategy was introduced on the basis of the sparse array configuration, enabling controlled beam steering while maintaining low sidelobe levels. **Figure 15** presents the directivity patterns after beam deflection using different beamforming methods.

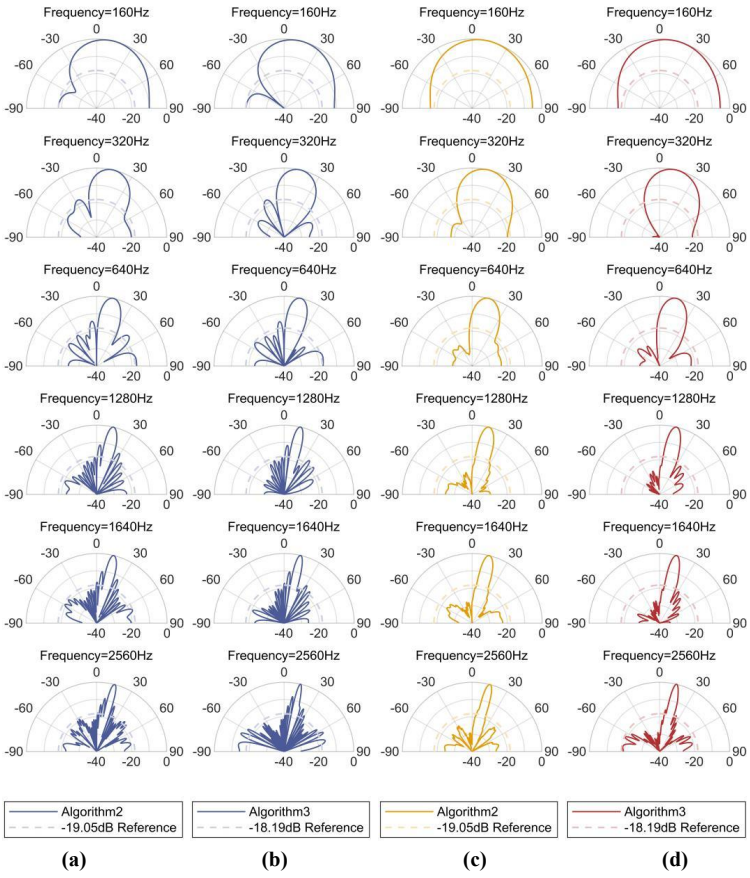

Figure 15. Comparison of beam steering directional patterns for the four proposed algorithms: **(a)** Beam steering directional pattern of **Algorithm 2**; **(b)** Beam steering directional pattern of **Algorithm 3**; **(c)** Beam steering directional pattern of **Algorithm 2** combined with the improved Cosh algorithm; **(d)** Beam steering directional pattern of **Algorithm 3** combined with the improved Cosh algorithm.

Simulation results indicate that, following optimization with the combined algorithm, the loudspeaker line array can effectively achieve directional steering of the main lobe while exhibiting significant sidelobe suppression. As the frequency increases, the sidelobe suppression performance is further enhanced, demonstrating good frequency response adaptability. The proposed combined algorithm not only preserves the main-lobe directivity of the array but also improves the beam's reconfigurability and broadband operational capability, addressing the issue of energy dispersion caused by elevated sidelobes during beam steering. This approach effectively reduces sidelobe levels and substantially enhances the spatial focusing of acoustic energy within the target region, thereby improving the overall acoustic performance of the array system.

5. Conclusion

In practical sound reinforcement applications, loudspeaker line arrays often exhibit periodic sidelobes due to their discrete structure, leading to spatial dispersion of acoustic energy. To address this issue, this study proposes an optimization approach based on sparse array design, aiming to effectively suppress sidelobe energy leakage while preserving the main-lobe performance. By sparsely configuring a subset of array elements and constructing a fitness function with the maximum sidelobe level as the objective, the element positions within the array geometry are optimized using both PSO and constrained GA. Engineering constraints, such as retaining elements at the array ends and maintaining structural symmetry, are incorporated to enable beam steering of the non-uniform sparse line array without mechanical movement. Simulation results demonstrate that, with the number of elements reduced from 40 to 34, both optimization methods achieve well-defined main lobes and significant sidelobe suppression. Notably, the PSO method exhibits faster convergence and superior sidelobe control, reducing the maximum sidelobe to −19.05 dB, while the GA also delivers favorable results under the imposed constraints, maintaining the maximum sidelobe below −18.19 dB. These findings confirm the effectiveness of the proposed approach in enhancing sound field focusing and energy control.

Building upon the sparse array structure, a combined algorithm is further introduced to achieve efficient beam steering while significantly lowering sidelobe levels, thereby improving array directivity and acoustic radiation performance. The sparse line array not only benefits from structural simplification but also leverages flexible phase and amplitude control to enhance beam steerability, enabling dynamic directional control in practical acoustic environments.

In summary, sparse optimization technology not only effectively reduces the number of array elements, thereby lowering system complexity and cost, but also maintains excellent directivity performance across multiple critical frequency bands. This technical solution offers an efficient and practical approach for deploying loudspeaker line arrays in venues such as theaters, stadiums, and multipurpose halls. However, several areas warrant further exploration. First, a Pareto frontier can be constructed that simultaneously considers main lobe width and side lobe level to achieve an optimal trade-off between main lobe width and side lobe sound

pressure level. Therefore, the core theme for future research expansion could be "multi-objective, multi-parameter optimization of main lobe width and side lobe sound pressure level". Secondly, the results presented herein primarily aim to illustrate the differences in convergence behavior between genetic algorithms (GA) and particle swarm optimization (PSO) as array dimensions increase. To comprehensively evaluate computational complexity and memory requirements, systematic statistical studies involving larger arrays, broader frequency ranges, and repeated experiments are necessary. Future research may further explore the potential of sparse arrays in three-dimensional configurations, adaptive control, and multi-objective optimization, aiming to enhance their robustness and intelligence in complex acoustic environments.

Author contributions: Conceptualization, YL and HR; methodology, YL; validation, ZL and QZ; investigation, YL; writing—original draft preparation, YL; writing—review and editing, HR, ZL and QZ; supervision, HR and ZL; project administration, HR. All authors have read and agreed to the published version of the manuscript.

Funding: This research was funded by the National Key Research and Development of China, grant number 2024YFF0907500.

Institutional review board statement: Not applicable.

Informed consent statement: Not applicable.

Data availability statement: Data sharing is not applicable to this article as no datasets were generated or analysed during the current study.

Conflict of interest: The authors declare no conflict of interest.

References

1. Wolff I, Malter L. Directional radiation of sound. The Journal of the Acoustical Society of America. 1930; 2(2): 201–241.
2. Ahrens J, Spors S. Sound field reproduction using planar and linear arrays of loudspeakers. IEEE Transactions on Audio, Speech, and Language Processing. 2010; 18(8): 2038–2050.
3. Bai MR, Hsieh YH. Point focusing using loudspeaker arrays from the perspective of optimal beamforming. The Journal of the Acoustical Society of America. 2015; 137(6): 3393–3410.
4. Mabande E, Kellermann W. Towards superdirective beamforming with loudspeaker arrays. In: Proceedings of the International Congress on Acoustics; 2–7 September 2007; Madrid, Spain.
5. Hao X, Wang Y, Zhang Y, et al. An optimization method for frequency-invariant beamforming with arbitrary sensor arrays. Applied Acoustics. 2023; 207: 109328.
6. Chen X, Zhang H, Lv Y. Improving the beamforming performance of a vector sensor line array with a coprime array configuration. Applied Acoustics. 2023; 207: 109329.
7. Wu X, Lee WN. Directional coherence factor for volumetric ultrasound imaging with matrix arrays. IEEE Transactions on Ultrasonics, Ferroelectrics, and Frequency Control. 2025; 72(6): 817–827.
8. Luo T, Yang W, Che W. High efficiency wide-beam antenna array with h-plane beamwidth enlargement and filtering properties for millimeter-wave applications. Microwave and Optical Technology Letters. 2025; 67(8): e70348.
9. Zhu Y, Zhang Y, Fan F, et al. An enhanced beamsteering algorithm based on mvdr for a multi-channel parametric array loudspeaker array. Journal of Sound and Vibration. 2025; 595: 118768.
10. Van Trees HL. Optimum Array Processing: Part IV of Detection, Estimation, and Modulation Theory. Wiley-Interscience; 2002.
11. Romoli L, Cecchi S, Peretti P, et al. Real-time implementation and performance evaluation of digital control for

loudspeakers line arrays. Applied Acoustics. 2015; 97: 121–132.
12. Gölles L, Zotter F, Merkel L. Miniature line array for immersive sound reinforcement. In: Proceedings of the AES 2023 International Conference on Spatial and Immersive Audio; 23–25 August 2023; Huddersfield, UK.
13. Møller MB, Martinez J, Østergaard J. Reduced complexity for sound zones with subband block adaptive filters and a loudspeaker line array. The Journal of the Acoustical Society of America. 2024; 155(4): 2314–2326.
14. Mai H, Xie B, Jiang J, et al. Influence of the number of loudspeakers on the timbre in horizontal and mixed-order ambisoncis reproduction. Sound & Vibration. 2019; 53(3): 112–125.
15. Jiang J, Xie B, Mai H. A comparison on the localization performance of static and dynamic binaural ambisonics reproduction with different order. Sound & Vibration. 2019; 53(1): 45–60.
16. Yan M, Chan CA, Gygax AF, et al. Efficient generation of optimal UAV trajectories with uncertain obstacle avoidance in MEC networks. IEEE Internet of Things Journal. 2024; 11(23): 38380–38392.
17. Yan M, Zhang Y, Chan CA, et al. Secure task offloading strategy optimization of UAV-aided outdoor mobile high-definition live streaming. Chinese Journal of Aeronautics. 2025; 38(10): 103454.
18. Yang S, Wang H, Xu Y, et al. A coupled simulated annealing and particle swarm optimization reliability-based design optimization strategy under hybrid uncertainties. Mathematics. 2023; 11(23): 4790. doi: 10.3390/math11234790
19. Yang S, Meng D, Keshtegar B, et al. ASVR-GPSO: A novel hybrid active support vector regression and global-best partial swarm optimization for structural reliability analysis. Structural and Multidisciplinary Optimization. 2025; 68(10). doi: 10.1007/s00158-025-04134-4
20. Xue H, Zhang X, Guo X, et al. Optimization of a random linear ultrasonic therapeutic array based on a genetic algorithm. Ultrasonics. 2022; 124: 106751.
21. Haupt RL. Thinned arrays using genetic algorithms. IEEE Transactions on Antennas and Propagation. 1994; 42(7): 993–999.
22. Pueo B, Escolano J, Roma M. Precise control of beam direction and beamwidth of linear loudspeaker arrays. In: Proceedings of the Workshop Proceedings, 2004 Sensor Array and Multichannel Signal; 18–21 July 2004; Barcelona, Spain. pp. 538–541.
23. Huang Z, Ma S, Wang H, et al. A uniform SPL distribution method of linear phased loudspeaker array using genetic algorithm. In: Proceedings of the 2012 IEEE 14th International Conference on Communication Technology; 9–11 November 2012; Chengdu, China. pp. 976–980.
24. Jin W, Kleijn WB. Theory and design of multizone soundfield reproduction using sparse methods. IEEE/ACM Transactions on Audio, Speech, and Language Processing. 2015; 23(12): 2343–2355.
25. Zhong J, Zhuang T, Li M, et al. Sidelobe suppression for a steerable parametric source using the sparse random array technique. IEEE/ACM Transactions on Audio, Speech, and Language Processing. 2023; 31: 3152–3161.
26. Khodier MM, Christodoulou CG. Linear array geometry synthesis with minimum sidelobe level and null control using particle swarm optimization. IEEE Transactions on Antennas and Propagation. 2005; 53(8): 2674–2679.
27. Ureda MS. Analysis of loudspeaker line arrays. Journal of the Audio Engineering Society. 2004; 52(5): 467–495.
28. Dawoud MM, Tennant A, Anderson AP. Array pattern nulling by element position perturbations using a genetic algorithm. Electronics Letters. 1994; 30(3): 174–176.
29. Chen K, He Z, Han C. A modified real GA for the sparse linear array synthesis with multiple constraints. IEEE Transactions on Antennas and Propagation. 2006; 54(7): 2169–2173.
30. Brown AD. Electronically Scanned Arrays MATLAB® Modeling and Simulation. CRC Press; 2017.
31. Krishna MV, Raju GSN, Mishra S. Sidelobe level reduction in linear antenna array synthesis using Cuckoo Search & Accelerated Particle Swarm algorithms. In: Proceedings of the 2016 International Conference on ElectroMagnetic Interference & Compatibility (INCEMIC); 14–16 December 2016; Bangalore, India. pp. 1–4.